Selective contribution of the twin-arginine translocation pathway to protein secretion in Bacillus subtilis

Jongbloed, JDH; Antelmann, H; Hecker, M; Bron, S; Airaksinen, U; Pries, F; Quax, WJ; van Dijl, JM; Braun, PG

Published in:
The Journal of Biological Chemistry

DOI:
10.1074/jbc.M203191200

Publication date:
2002

THE JOURNAL OF BIOLOGICAL CHEMISTRY
Vol. 277, No. 46, Issue of November 15, pp. 44068–44078, 2002
Printed in U.S.A.

Selective Contribution of the Twin-Arginine Translocation Pathway to Protein Secretion in *Bacillus subtilis**

Received for publication, April 3, 2002, and in revised form, August 27, 2002
Published, JBC Papers in Press, September 5, 2002, DOI 10.1074/jbc.M203191200

Jan D. H. Jongbloed‡§, Haike Antelmann§¶, Michael Hecker¶, Reindert Nijland‡, Sierd Bron‡, Ulla Airaksinen‖, Frens Pries‡‡, Wim J. Quax‡‡, Jan Maarten van Dijl‡‡§§, and Peter G. Braun‡‡**

From the ‡Department of Genetics, Groningen Biomolecular Sciences and Biotechnology Institute, Kerklaan 30, 9751 NN Haren, The Netherlands, the ¶Institut für Mikrobiologie und Molekularbiologie, Ernst-Moritz-Arndt-Universität Greifswald, F.-L.-Jahn-Strasse 15, D-17487 Greifswald, Germany, the ‖National Public Health Institute, Mannerheimintie 166, FIN-00300, Helsinki, Finland, and the ‡‡Department of Pharmaceutical Biology, University of Groningen, A. Deusinglaan 1, 9713 AV Groningen, The Netherlands

The availability of the complete genome sequence of *Bacillus subtilis* has allowed the prediction of all exported proteins of this Gram-positive eubacterium. Recently, ~180 secretory and 114 lipoprotein signal peptides were predicted to direct protein export from the cytoplasm. Whereas most exported proteins appear to use the Sec pathway, 69 of these proteins could potentially use the Tat pathway, as their signal peptides contain RR- or KR-motifs. In the present studies, proteomic techniques were applied to verify how many extracellular *B. subtilis* proteins follow the Tat pathway. Strikingly, the extracellular accumulation of 13 proteins with potential RR/KR-signal peptides was Tat-independent, showing that their RR/KR-motifs are not recognized by the Tat machinery. In fact, only the phosphodiesterase PhoD was shown to be secreted in a strictly Tat-dependent manner. Sodium azide-inhibition of SecA strongly affected the extracellular appearance of *de novo* synthesized proteins, including the lipase LipA and two other proteins with predicted RR/KR-signal peptides. The SecA-dependent export of pre-LipA is particularly remarkable, because its RR-signal peptide conforms well to stringent criteria for the prediction of Tat-dependent export in *Escherichia coli*. Taken together, our observations show that the Tat pathway makes a highly selective contribution to the extracellular proteome of *B. subtilis*.

The Gram-positive soil bacterium *Bacillus subtilis*, is well known for its ability to secrete a large variety of proteins into its extracellular environment. Based on the complete genome sequence (1), it was recently predicted that the extracellular proteome of this organism is composed of ~180 different proteins (2, 3). Indeed, a two-dimensional gel electrophoretic analysis showed that about 200 distinct spots representing extracellular proteins can be separated, among which 82 different proteins were identified (4). To date, it is not known to what extent each of the various known protein export pathways contributes to the composition of the extracellular proteome.

Four pathways for protein export are known to be present in *B. subtilis*. As judged by the characteristic tripartite structure of their signal peptides, the majority of secretory proteins (~160) has the potential to be exported from the cytoplasm via the Sec (protein secretion) pathway (2, 3). In addition, this pathway is required for the export of 114 potential lipoproteins that remain anchored to the cytoplasmic membrane (5). Notably, some of these lipoproteins are released into the growth medium by secondary processing events (4). In contrast, small numbers of proteins are exported via the dedicated pseudopilin export pathway (Com) for competence development (~4) and ATP-binding cassette (ABC) transporters (~4) (2, 3). Importantly, the number of proteins exported via the Tat[1] (twin-arginine translocation) pathway of *B. subtilis* was, so far, difficult to estimate on the basis of signal peptide predictions (6).

Typical twin-arginine (RR) signal peptides that direct Tat-dependent protein export in Gram-negative bacteria, such as *Escherichia coli*, or Tat-dependent protein import into the thylakoid lumen of chloroplasts, are characterized by the presence of a so-called "twin-arginine" consensus motif (RRX$\phi\phi$, where ϕ is a hydrophobic residue). In this RR-motif, the twin-arginines and the hydrophobic residues at the +2 and +3 positions were shown to be important for Tat-dependent export. Furthermore, it was reported that these RR-signal peptides are generally longer and less hydrophobic than Sec-type signal peptides (7–11). Strikingly, however, the first arginine residue of the typical RR-pair, which was initially believed to be invariant, could be substituted for a lysine residue without blocking the Tat-dependent export of the *E. coli* SufI protein (12). Moreover, naturally occurring KR-signal peptides, in which the first of the two invariant arginine residues was replaced with a lysine residue, were shown to direct the Tat-dependent translocation of the *Salmonella enterica* TtrB protein and the *Spinacia oleracea* Rieske Fe/S protein (13, 14). Even an RNR-signal peptide was recently shown to direct a pre-pro-penicillin amidase into the Tat pathway of *E. coli* (15). The discovery of these

* This work was supported in part by "Quality of Life and Management of Living Resources" Grants QLK3-CT-1999-00413 and QLK3-CT-1999-00917 from the European Union (to J. D. H. J., H. A., M. H., P. G. B., S. B., W. J. Q., and J. M. v. D) and grants from the "Deutsche Forschungsgemeinschaft" (DFG), the "Bundesministerium für Bildung, Wissenschaft, Forschung und Technologie" (BMFT), the "Fonds der Chemischen Industrie," and Genencor International (to H. A. and M. H). The costs of publication of this article were defrayed in part by the payment of page charges. This article must therefore be hereby marked "*advertisement*" in accordance with 18 U.S.C. Section 1734 solely to indicate this fact.

§ These authors contributed equally to this work.
** Present address: IPSAT Therapies Ltd., Koetilantie 5, FIN-00710, Helsinki, Finland.
§§ To whom correspondence should be addressed. Tel.: 31-50-3633079; Fax: 31-50-3633000; E-mail: j.m.van.dijl@farm.rug.nl.

[1] The abbreviations used are: Tat, twin-arginine translocation; IPTG, isopropyl-β-D-thiogalactopyranoside; IPG, immobilized pH gradient; MALDI-TOF, matrix-assisted laser desorption/ionization-time of flight; Km, kanamycin.

atypical RR-signal peptides shows that the prediction of signal peptides that direct Tat-dependent protein transport cannot be based exclusively on the presence of twin-arginine residues. This view is underscored by our recent two-dimensional gel electrophoretic analysis of the *B. subtilis* proteins that are exported under conditions of phosphate starvation. Of the four detected proteins with an RR-motif in their signal peptide only one, the phosphodiesterase PhoD, was exported in a strictly Tat-dependent manner (6).

The presently best characterized bacterial Tat translocase is that of *E. coli*. In contrast to the Sec translocase, which facilitates the export of loosely folded proteins only, the Tat translocase allows the passage of fully folded proteins across the inner membrane (for a recent review see Ref. 16). The key components for twin-arginine translocation are the integral membrane proteins TatA, TatB, and TatC (17–20). The TatA paralogue TatE has overlapping functions with TatA, but TatA appears to be far more important for translocation than TatE. In contrast to *E. coli* and most other eubacteria, which contain only one *tatC* gene, *B. subtilis* contains two *tatC* genes (denoted *tatCd* and *tatCy*). The TatCd protein was shown to be specifically involved in the export of the RR-protein PhoD, unlike its paralogue TatCy (6). Each of the *tatC* genes is preceded by a *tatA* gene (denoted *tatAd* and *tatAy* respectively). A third *tatA* gene (*tatAc*) is not genetically linked to the *tatC* genes. Notably, the three *B. subtilis* TatA proteins show sequence similarity with both the *E. coli* TatA/E and TatB proteins (6). It is presently not known to what extent the *B. subtilis* TatA proteins are functionally equivalent to the *E. coli* TatA/E or TatB proteins.

The present studies were aimed at answering the question to what extent the Tat pathway of *B. subtilis* contributes to the extracellular accumulation of proteins. For this purpose, the extracellular proteomes of multiple *tat* mutant strains were analyzed by two-dimensional gel electrophoresis and mass spectrometry. The results show that out of 69 candidate proteins with RR- and KR-signal peptides (Table I), only one protein is secreted in a strictly Tat-dependent manner, whereas 13 other proteins that can be visualized by proteomic techniques are secreted Tat-independently. In fact, the extracellular accumulation of three of these 13 proteins was shown to be Sec-dependent. The observation that the export of LipA[2] is Sec- and not Tat-dependent was salient, because its RR-motif conforms to the most stringent criteria for the prediction of RR/KR-signal peptides that direct Tat-dependent export.

EXPERIMENTAL PROCEDURES

Plasmids, Bacterial Strains and Media—Table II lists the plasmids and bacterial strains used. Rich medium contained Bacto tryptone (1%), Bacto yeast extract (0.5%), and NaCl (1%). Minimal medium (MM) was prepared as previously described (21). Schaeffer's sporulation medium (SSM) was prepared as described by Schaeffer *et al.* (22). High phosphate (HPDM)- and low phosphate (LPDM)-defined media were prepared as described by Müller *et al.* (23). When required, media for *E. coli* were supplemented with ampicillin (Ap; 100 μg/ml), erythromycin (Em; 100 μg/ml), kanamycin (Km; 40 μg/ml), chloramphenicol (Cm; 5 μg/ml), or spectinomycin (Sp; 100 μg/ml); media for *B. subtilis* were supplemented with Em (1 μg/ml), Km (10 μg/ml), Cm (5 μg/ml), and/or Sp (100 μg/ml).

DNA Techniques—Procedures for DNA purification, restriction, ligation, agarose gel electrophoresis, and transformation of *E. coli* were carried out as described by Sambrook *et al.* (24). Enzymes were from Roche Molecular Biochemicals, Invitrogen, or New England Biolabs. *B. subtilis* was transformed as previously described (21). PCR was carried out with the *Pwo* DNA polymerase (New England Biolabs) as described (25).

To construct *B. subtilis* Δ*tatCd*(Cm), the *tatCd* gene was amplified by PCR with primer JJ33Cdd (5′-GGA ATT CGT GGG ACG GCT ACC-3′) containing an *Eco*RI site and 5′-sequences of *tatCd*, and primer JJ34Cdd (5′-CGG GAT CCA TCA TGG GAA GCG-3′) containing a *Bam*HI site and 3′-sequences of *tatCd*. Next, the PCR-amplified fragment was cleaved with *Eco*RI and *Bam*HI and ligated into the corresponding sites of pUC21, resulting in pJCd1. Plasmid pJCd3 was obtained by ligating a pUC7C-derived Cm resistance marker, flanked by *Bam*HI restriction sites, into the unique *Bcl*I site of the *tatCd* gene in pJCd1. Finally, *B. subtilis* Δ*tatCd*(Cm) was obtained by a double crossover recombination event between the disrupted *tatCd* gene of pJCd3 and the chromosomal *tatCd* gene. The double *tatCy-tatCd*(Cm) mutant was constructed by transforming the Δ*tatCy* mutant (6) with chromosomal DNA of the Δ*tatCd*(Cm) mutant strain. Correct integration of resistance markers into the chromosome of *B. subtilis* was verified by Southern blotting or PCR. This was also done for all integrations described below.

To construct *B. subtilis* Δ*tatAc*, the *tatAc* gene was amplified by PCR with primer JJ45Acd (5′-GGA ATT CAG AAA GTC TGG GAG-3′) containing an *Eco*RI site and 5′-sequences of *tatAc*, and primer JJ46Acd (5′-GCT CTA GAA ATA TAC ATA TAG TGC-3′) containing an *Xba*I site and 3′-sequences of *tatAc*. Next, the PCR-amplified fragment was cleaved with *Eco*RI and *Xba*I and ligated into the *Eco*RI and *Xba*I sites of pUK21, resulting in pJKAc1. Plasmid pJKAc4 was obtained by ligating a pDG646-derived Em resistance marker, flanked by *Hin*dIII restriction sites, into the unique *Hin*dIII site of the *tatAc* gene in pJKAc1. Finally, *B. subtilis* Δ*tatAc* was obtained by a double crossover recombination between the disrupted *tatAc* gene of pJKAc4 and the chromosomal *tatAc* gene (Fig. 1).

To construct a *B. subtilis* mutant lacking the *tatAy-tatCy* operon (Δ*tatAyCy*), two DNA fragments containing 5′-sequences of *tatAy* and 3′-sequences of *tatCy* respectively, were amplified by PCR. The 5′-fragment of *tatAy* was amplified with primer JJ49Ayd (5′-GGG GTA CCT TAA AGA ATC TGC ATG CG-3′), which contains a *Kpn*I site and sequences upstream of *tatAy*, and primer RN03 (5′-GGC CCA AGC TTC CAG GAC CGA TCG G-3′), which contains a *Hin*dIII site and codons 4–21 of the *tatAy* gene. The 3′-fragment of *tatCy* was amplified with primer RN04 (5′-CTC CCA AGC TTA TCG GAA AGC ACA GAA AAG C-3′), which contains a *Hin*dIII site and codons 706–729 of the *tatCy* gene, and primer JJ30Cyd (5′-CGG GAT CCT TTG GGC GAT AGC C-3′), which contains a *Bam*HI site and sequences downstream of *tatCy*. Next, these PCR-amplified fragments were cleaved with *Kpn*I/*Hin*dIII and *Hin*dIII/*Bam*HI, respectively, and ligated into the *Asp*718 and *Bam*HI sites of pUC21. This resulted in pRACy1. Plasmid pRACy3 was obtained by ligating a pDG1726-derived Sp resistance marker, flanked by *Hin*dIII restriction sites, into the unique *Hin*dIII site of pRACy1, which is located between the 5′-sequences of *tatAy* and the 3′-sequences of *tatCy*. Finally, *B. subtilis* Δ*tatAyCy* was obtained by a double crossover recombination between the *tatAy-tatCy* region of pRACy3 and the chromosomal *tatAy-tatCy* operon (Fig. 1).

To construct a *B. subtilis* mutant (Δ*tatAdCd*) lacking the *tatAd-tatCd* operon, two DNA fragments containing 5′-sequences of *tatAd* and 3′-sequences of *tatCd*, respectively, were amplified by PCR. The 5′-fragment of *tatAd* was amplified with primer JJ47Add (5′-GGA ATT CCC AGA TAT CGA GCT GTA CC-3′), which contains an *Eco*RI site and sequences upstream of *tatAd*, and primer RN07 (5′-AGT TCG TAC GTT AGC GTC GAC CAA TGT TTG AAA ACA TAA TTT CC-3′), which contains an *Acc*I site and codons 1–17 of the *tatAd* gene. The 3′-fragment of *tatCd* was amplified with primer RN08 (5′-CCT CAT CCT CTT TTT GTC GAC GCT AAC GTA AGT ACT-3′), which contains an *Acc*I site and codons 698–714 of *tatCd*, and primer JJ34Cdd (5′-CGG GAT CCA TCA TGG GAA GCG G-3′), which contains a *Bam*HI site and sequences downstream of *tatCd*. Next, these PCR-amplified fragments were cleaved with *Eco*RI/*Acc*I and *Acc*I/*Bam*HI, respectively, and ligated into the *Eco*RI and *Bam*HI sites of pUC21. This resulted in pRACd1. Plasmid pRACd5 was obtained by ligating a pUC7C-derived Cm resistance marker, flanked by *Acc*I restriction sites, into the unique *Acc*I site of pRACd1, which is located between the 5′-sequences of *tatAd* and the 3′-sequences of *tatCd*. Finally, *B. subtilis* Δ*tatAdCd* was obtained by a double crossover recombination between the disrupted *tatAd-tatCd* region of pRACd5 and the chromosomal *tatAd-tatCd* operon (Fig. 1).

To construct the total-*tat* mutant, the Δ*tatAc* mutant was transformed with chromosomal DNA of the Δ*tatAyCy* mutant strain. The disruption of the *tatAy-tatCy* operon in the resulting Δ*tatAc*-Δ*tatAyCy* strain was verified by PCR. This triple mutant strain was then transformed with chromosomal DNA of the Δ*tatAdCd* mutant, resulting in the total-*tat* strain. The absence of all *tat* genes from the total-*tat* strain was verified by PCR.

[2] Please note that LipA is referred to as Lip in the SubtiList database (genolist.pasteur.fr/SubtiList/).

TABLE I

Predicted RR- and KR-signal peptides of B. subtilis

Putative RR- and KR-signal peptides were identified in two ways. First, the presence of the consensus sequence RRX$\phi\phi$ or KRX$\phi\phi$ (ϕ is a hydrophobic residue), immediately in front of an N-terminal hydrophobic region as predicted with the TopPred2 algorithm (45, 46), was determined. To this purpose, the first 60 residues of all annotated proteins of *B. subtills* in the SubtiList database (genolist.pasteur.fr/SubtiList/) were used. Second, within the group of potential RR/KR-sorting signals, cleavable signal peptides were identified with the SignalP algorithm (47, 48). Conserved residues of the consensus sequence (RRX$\phi\phi$ or KRX$\phi\phi$) are indicated in bold. In addition, positively charged residues that could function as a so-called Sec avoidance signal (49) are indicated in bold and italics. Note, however, that the positively charged residues in the signal peptides of LipA and YolA do not cause Sec avoidance. The hydrophobic H-domain is indicated in gray shading and the average hydrophobicity (h) of each of these domains, as determined by the algorithms of Kyte and Doolittle (50), is indicated. To calculate these hydrophobicities, the ProtScale Tool was used, which is available through the ExPASy server at *us.expasy.org/tools/pscale/Hphob.Doolittle.html.* Please note that the hydrophobicity scale values for different amino acids are dimension-less. In signal peptides with a predicted signal peptidase I cleavage site, residues from position −3 to −1 relative to the signal peptidase I cleavage site are underlined. Notably, some of these proteins contain one or more putative transmembrane segments elsewhere in the protein (indicated with "TM"), or are putative lipoproteins. Residues forming a so-called lipobox for signal peptidase II cleavage are enlarged in size (51). Proteins containing cell wall binding repeats in the mature part of the protein are indicated with "W."

protein	signal peptide	h
AlbB	MSPAQRRILLYILSFIFVIGAVVYFVKSDYLFTLIFIAIAILF	2.0
Amy	MVSIRRSFEAYVDDMNIITVLIPAEQKEIM	1.1
AppB^{TM}	MAAYIIRRTLMSIPILLGITILSFVIMKAAPGD	2.3
LipA	MKFVKRRIIALVTILMLSVTSLFALQPSAKAAEH	1.2
OppB^{TM}	MLKYIGRRLVYMIITLFVIVTVTFFLMQAAPGG	2.0
PbpX	MTSPTRRRTAKRRRRKLNKRGKLLFGLLAVMVCITIWNALHR	2.9
PhoD	MAYDSRFDEWVQKLKEESFQNNTFDRRKFIQGAGKIAGLSLGLTIAQSVGAFEV	0.9
QcrA	MGGKHDISRRQFLNYTLTGVGGFMAASMLMPMVRFALDP	1.3
SpoIIIJ^{TM}	MLLKRRIGLLLSMVGVFMLLAGCSSV	2.6
TlpA^{TM}	MKKTLTTIRRSSIARRLIISFLLILIVPITALSVSAYQSAVAS	2.4
WapA^{W}	MKKRKRRNFKRFIAAFLVLALMISLVPADVLAKST	2.3
WprA	MKRRKFSSVVAAVLIFALIFSLFSPGTKAAAAGA	1.9
YceA^{TM}	MEMFDLEFMRRAFLAGGMIAVMAPILGVYLVLRRQALM	2.2
YdeJ	MKKRRKICYCNTALLLMILLAGCTDS	2.1
YdhF	MRRILSILVFAIMLAGCSSN	3.1
YdhK	MSAGKSYRKKMKQRRMNMKISKYALGILMLSLVFVLSACGNN	2.5
YesM^{TM}	MKKRVAGWYRRMKIKDKLFVFLSLIMAVSFLFVYSGVQYAFHV	2.4
YesW	MRRSCLMIRRKRMFTAVTLLVLLVMGTSVCPVKAEGA	2.0
YfkN^{TM}	MRIQKRRTHVENILRILLPPIMILSLILPTPPIHAEES	1.7
YhcR^{TM}	MLSVEMISRQNRCHYVYKGGNMMRRILHIVLITALMFLNVMYTFEAVKA	2.0
YkpC	MLRDLGRRVAIAAILSGIILGGMSISLANMP	2.3
YkuE	MKKMSRRQFLKGMFGALAAGALTAGGGYGYARYL	1.0
YmaC	MRRFLLNVILVLAIVLFLRYVHYSLEPE	2.4
YmzC	MFESEAELRRIRIALVWIAVFLLFGACGN	3.1
YubF^{TM}	MQKYRRRNTVAFTVLAYFTFFAGVFLFSIGLYNADNLE	2.0
YuiC	MMLNMIRRLLMTCLFLLAFGTTFLSVSGIEAKDL	1.9
YvhJ^{TM}	MAERVRVRVRKKKKSKRRKILKRIMLLFALALLVVVGLGGYKLY	2.5
YwbN	MSDEQKKPEQIHRRDILKWGAMAGAAVAIGASGLGGLAPLVQTAAKP	1.4
AbnA^{W}	MKKKKTWKRFLHFSSAALAAGLIFTSAAPAEAAFW	1.4
AspB	MKLAKRVSALTPSTTLAITAKAKEL	1.1
BglC	MMRRRKRSDMKRSISIFITCLLITLLTMGGMIASPASAAGT	1.8
BglS	MPYLKRVLLLLVTGLFMSLFAVTATASAQTG	2.3
DacF	MKRLLSTLLIGIMLLTFAPSAFAKQD	2.0
DltD	MKKRFFGPIILAPILFAGAIAIPS	2.4
LytD^{W}	MKKRLIAPMLLSAASLAFFAMSGSAQAAAY	1.7
MreC	MPNKRLMLLLLCIIILVAMIGFSLKG	3.5
OppA	MKKRWSIVTLMLIFTLVLSACGFG	2.3
OpuBC	MKRKYLKLMIGLALAATLTLSGCSLPGLSAAADQ	1.8
PelB	MKRLCLWFTVFSLFLVLLPGKALGAVD	1.9
PhrG	MKRFLIGAGVAAVILSGWFIADHQ	2.0
SacC	MKKRLIQVMIMFTLLLTMAFSADAADS	2.1
SpoIIQ	MREEEKKTSQVKKLQQFFRRRWVFPAIYLVSAAVILTAVLWYQ	2.0
WapA^{W}	MKKRKRRNFKRFIAAFLVLALMISLVPADVLAKST	2.3
YckD	MKRITINIITMFIAAAVISLTGTAEAAEK	1.9
YddT	MRKKRVITCVMAASLTLGSLLPAGYASAKED	1.6
YdjN	MKKRIILLLAVIIAAAAAGVAFYV	3.2
YjfA	MKRLFMKASLVLFAVVFVFAVKGAPAKAETH	2.1
YkrL^{TM}	MAKRIFLFILTNILVLTTIGIVLSVLSSVTGVGTYFT	2.2
YkvV	MLTKRLLTIYIMLLGLIAWFPGAAQAEEK	2.0
YndF	MKSKLKRQLPAMVIVCLLMICVTGCWSS	2.9
YocA	MKKRRKGCFAAAGFMMIFVFVIASFL	2.2
YolA	MKKRITYSLLALLAVVAFAFTDSSKAKAAEA	1.4
YolC	MKKRLIGFLVLVPALIMSGITLIEANKK	2.4
YomL	MRKKRVITCVMAASLTLGSLLPAGYATAKED	1.6
YoqH	MKRFILVLSFLSIIVAYPIQTNASPM	2.2
YozF	MKRVLFSVIVFTAVGFTFCQSK	2.6
YpmS	MNKWKRLFFILLAINFILAAGFVALVLLPGEQAQVKDA	2.1
YqfZ	MKRLTLVCSIVFILFILFYDLKIGTIPIQDLPVYEASAKTA	1.5
YqzC	MTKRGIQAFAGGIILATAVLAAVFYLTDEDQAAAVKD	1.1
YrpE	MNILFSKRLGILTIGSLLVLAGCQTS	2.4
YrrL	MYINQQKKSFFNKKRIILSSIVVLFLIIGGAFLYGK	2.9
YtmJ	MNKRKGLVLLLSVFALLGGGCSQT	2.9
YunB	MPRYRGPFRKRGPLPFRYVMLLSVVFFILSTTVSLWMI	1.4
YutC	MKRTAVSLCLLTGLLSGCGGA	1.9
YvgO	MKRIRIPMTLALGAALTIAPLSFASAEEN	1.7
YvrC	MKKRAGIWAALLLAAVMLAGCGNP	2.3
YwcI	MKRLLVSLRVWMVFLMNWVTPDRKTARAAVY	0.6
YwmC	MKKRFSLIMMTGLLFGLTSPAFAAEKT	1.5
YxkH	MKRLFLSIFLLGSCLALAACADQ	2.4
YyaB	MVYQTKRDVPVTLMIVFLILLIQADAIVP	2.7

TABLE II
Plasmids and Strains

Plasmids	Relevant properties	Ref.
pUC21	cloning vector; 3.2 kb; Ap^r	52
pUK21	cloning vector; 3.1 kb; Km^r	52
pJCd1	pUC21 derivative; carrying the *tatCd* gene; 5.4 kb; Ap^r	6
pJCd3	pUC21 derivative for the disruption of *tatCd*; 6.4 kb; Cm^r; Ap^r	This work
pJKAc1	pUK21 derivative; carrying the *tatAc* gene; 4.8 kb; Km^r	This work
pJKAc4	pUK21 derivative for the disruption of *tatAc*; 6.4 kb; Km^r; Em^r	This work
pRACd1	pUC21 derivative; carrying the *tatAd-tatCd* operon; 4.7 kb; Ap^r	This work
pRACd5	pUC21 derivative for the replacement of the *tatAd-tatCd* operon; 5.7 kb; Ap^r; Cm^r	This work
pRACy1	pUC21 derivative; carrying the *tatAy-tatCy* operon; 4.6 kb; Ap^r	This work
pRACy3	pUC21 derivative for the replacement of the *tatAy-tatCy* operon; 5.8 kb; Ap^r; Sp^r	This work
pLip2031	pUB110 derivative; carries the *B. subtilis lipA* gene under the control of the HpaII promoter; 4.6 kb; Km^r	38
pKTH10	encodes the α-amylase (AmyQ) of *B. amyloliquefaciens*, 6.8 kb; Km^r	53
pMutin2	pBR322-based integration vector for *B. subtills;* containing a multiple cloning site downstream of the P_{spac} promoter, and a promoter-less *lacZ*-gene preceded by the RBS of the *spoVG* gene; 8.6 kb; Ap^r; Em^r	54
pUC7C	contains a Cm resistance cassette; 3.7 kb; Ap^r; Cm^r	Lab collection
pDG646	contains an Em resistance cassette; 4.0 kb; Ap^r; Em^r	55
pDG1726	contains a Sp resistance cassette; 3.9 kb; Ap^r; Sp^r	55
Strains		
E. coli		
MC1061	*F:araD*139; Δ (*ara-leu*)7696; Δ (*lac*)X74; *galU; galK; hsdR2; mcrA: mcrB1; rspL:*	56
B. subtilis		
168	*trpC2*	1
Δ*tatCd*	*trpC2; tatCd*; Km^r	6
Δ*tatCd*(Cm)	*trpC2; tatCd;* Cm^r	This work
Δ*tatCy*	*trpC2; tatCy;* Sp^r	6
Δ*tatCd*-Δ*tatCy*	*trpC2; tatCd;* Km^r; *tatCy*; Sp^r	6
Δ*tatCy*-Δ*tatCd*(Cm)	*trpC2; tatCy*; Sp^r; *tatCd*; Cm^r	This work
Δ*tatAc*	*trpC2; tatAc*; Em^r	This work
Δ*tatAdCd*	*trpC2; tatAd-tatCd*; Cm^r	This work
Δ*tatAyCy*	*trpC2; tatAy-tatCy*; Sp^r	This work
Δ*tatAc*-Δ*tatAyCy*	*trpC2; tatAc*; Em^r; *tatAy-tatCy*; Sp^r	This work
total-*tat*	*trpC2; tatAc*; Em^r; *tatAy-tatCy*; Sp^r; *tatAd-tatCd*; Cm^r	This work
I*secA*	*trpC2*; P_{spac}-*secA; secA-lacZ*; Em^r	This work

To construct *B. subtilis* I*secA*, a fragment comprising the ribosome-binding site, start codon and the 5′-region of the *secA* gene, but not the *secA* promoter(s), was amplified with the primers secA1 (5′-GGA ATT CAT AGA GGA GCG TTA TAA AT-3′) and secA2 (5′-CGG GAT CCA TGC CTG TTA CGC GGC-3′). The amplified fragment was cleaved with *Eco*RI and *Bam*HI, and ligated into the corresponding sites of pMutin2, resulting in pMI-secA. *B. subtilis* I*secA* was obtained by Campbell-type integration of pMI-secA in the *secA* locus of *B. subtilis* 168, in such a way that the *secA* promoter region was replaced by the isopropyl-β-D-thiogalacto-pyranoside (IPTG)-dependent P*spac* promoter, whereas the *spoVG-lacZ* reporter gene of pMutin2 is under the transcriptional control of the *secA* promoter region.

Competence and Sporulation—Competence for DNA binding and uptake was determined by transformation with plasmid or chromosomal DNA (26). The efficiency of sporulation was determined by overnight growth in SSM medium, killing of cells with 0.1 volume of chloroform and subsequent plating.

Two-dimensional Gel Electrophoresis and Image Analysis—B. subtilis tat mutant strains and the parental strain 168 were grown at 37 °C under vigorous agitation in 1 liter of rich medium, or a synthetic medium containing 0.16 mM KH_2PO_4 to induce a phosphate starvation response (27). After 1 h of postexponential growth, cells were separated from the growth medium by centrifugation. The secreted proteins in the growth medium were precipitated overnight with ice-cold 10% TCA, collected by centrifugation (40,000 × *g*, 2 h, 4 °C), and further prepared for two-dimensional gel electrophoresis as described below. To study the effects of the SecA translocation ATPase inhibitor sodium azide on protein secretion, *B. subtilis* strain 168 was grown at 37 °C under vigorous agitation in 1 liter of rich medium to an OD_{540} of 3.0. Then, cells were harvested by centrifugation (5000 rpm, 5 min, room temperature) and washed twice with prewarmed rich medium. The washed cells were resuspended in 1 liter of prewarmed rich medium and, subsequently, divided into two aliquots of 500 ml, one of which was supplemented with sodium azide at a final concentration of 15 mM. The two resulting cultures were incubated under vigorous agitation and aliquots of 250 ml were harvested from each culture after 10 and 20 min, respectively. The proteins secreted into the medium within the 10 or 20 min periods of incubation were separated from the cells by centrifugation and trichloroacetic acid-precipitated as described above. Dried trichloroacetic acid-precipitated protein pellets were washed three times with 96% ethanol, dried, and resuspended in a solution containing 2 M thiourea and 8 M urea. Subsequently, insoluble material was removed by centrifugation. The protein concentration of the resulting samples was determined as decribed by Bradford (28), and 100 μg of the extracellular protein sample was adjusted to 360 μl with the thiourea/urea solution. Next, 40 μl of a 10-fold concentrated reswelling solution was added containing 2 M thiourea, 8 M urea, 10% Nonidet P-40 (v/v), 200 mM dithiothreitol, and 5% Pharmalyte 3–10. This sample was used for the rehydration of immobilized pH gradient strips (pH 3–10; Amersham Biosciences). Isoelectric focusing was performed using the Multiphor II unit (Amersham Biosciences) and SDS-polyacrylamide gel electrophoresis (PAGE) in the second dimension was carried out using the Investigator two-dimensional electrophoresis system (Genomic Solutions, Chelmsford, MA) as described previously (4). The resulting two-dimensional gels were fixed with 50% (v/v) methanol, 7% (v/v) acetic acid and stained with SYPRO Ruby protein gel stain (Molecular Probes Inc.). Fluorescence was detected using a Storm860 fluorescence imager.

Two-dimensional gel image analysis was performed with the DECODON Delta 2D software (www.decodon.com), which is based on dual channel image analysis (29). Using this software the master image (represented by green spots) is warped with the sample image (represented by red spots) after setting specific vector points. Consequently, green protein spots in the dual channel image are predominantly present in the master image, while red protein spots are predominantly present in the sample image. Yellow protein spots are present at similar amounts in both images. After background subtraction, a normalization is performed in order to equalize the gray values in each image. Each experiment was repeated at least three times.

Protein Identification—In-gel tryptic digestion of proteins, separated by two-dimensional gel electrophoresis, was performed using a peptide-collecting device (30). The peptide solution (0.5 μl) was mixed with an equal volume of a saturated α-cyano-4-hydroxy cinnamic acid solution in 50% acetonitrile and 0.1% trifluoroacetic acid. The resulting mixture was applied to the sample template of a matrix-assisted laser desorption/ionisation (MALDI) - time of flight (TOF) mass spectrometer (Voy-

ager DE-STR, PerSeptive Biosystems). Peptide mass fingerprints were analyzed using the MS-Fit software, as provided by Baker and Clausner through prospector.ucsf.edu.

Western Blot Analysis—To detect LipA, *B. subtilis* cells were separated from the growth medium by centrifugation (2 min, 13,000 × *g*, room temperature). Proteins in the growth medium were concentrated 20-fold upon precipitation with trichloroacetic acid, and samples for SDS-PAGE were prepared as described previously (31). After separation by SDS-PAGE, proteins were transferred to a polyvinylidene-difluoride membrane (Molecular Probes Inc.), and LipA was visualized with specific antibodies and horseradish peroxidase-conjugated goat anti-rabbit antibodies (Sigma) according to the manufacturer's instructions.

N-terminal Sequencing—To determine the N-terminal amino acid sequence of mature LipA, *B. subtilis* cells were separated from the growth medium by two subsequent centrifugation steps (3 min, 13,000 × *g*, room temperature). Proteins in the growth medium were concentrated 20-fold upon precipitation with trichloroacetic acid, and samples for SDS-PAGE were prepared as indicated in the Perkin Elmer user bulletin no. 58. After separation by SDS-PAGE, proteins were transferred to a polyvinylidene difluoride membrane (Schleicher and Schuell) and stained with Coomassie Brilliant Blue. The protein band corresponding to mature LipA was excised and used to determine the N-terminal amino acid sequence by automated Edman degradation with the Protein Sequencer 476A (Perkin Elmer Co.).

Lipase Activity Assay—To determine lipase (*i.e.* esterase) activity, the colorimetric assay as described by Lesuisse *et al.* (32) was applied with some modifications. In short, 900 μl of reaction buffer (0.1 M H_2KPO_4, pH 8.0, 0.1% arabic gum, 0.36% Triton X-100) was supplemented with 50 μl of the chromophoric ligand 4-nitrophenyl caprylate (10 mM in methanol). The reaction was started by the addition of 50 μl of culture supernatant. Lipase activity was determined by measuring the increase in the absorbance at 405 nm per min of incubation at 30 °C, per OD_{600} of the culture at the time of sampling.

Pulse-Chase Protein Labeling, Immunoprecipitation, SDS-PAGE, and Fluorography—Pulse-chase labeling of *B. subtilis*, immunoprecipitation, SDS-PAGE, and fluorography were performed as described previously (33, 34). To inhibit the translocation ATPase activity of SecA, sodium azide (1.5 mM) was added to the cells 5 min prior to labeling (35). Immunoprecipitations were performed with specific antibodies against LipA, AmyQ, SecA, or GroEL.

RESULTS

Construction of a B. subtilis Total-tat Mutant—Previous analysis of the extracellular proteome of the Δ*tatCd*-Δ*tatCy* mutant strain, grown under the conditions of phosphate starvation, showed that the secretion of the phosphodiesterase PhoD, which is synthesized with an RR-signal peptide, was completely blocked by the *tatC* double mutation (6). In contrast, the secretion of the WprA, YdhF, and YfkN proteins was not affected by the disruption of the two *tatC* genes, despite the presence of an RR-motif in their signal peptides. To exclude the possibility that the Δ*tatCd*-Δ*tatCy* mutant is leaky for certain RR-preproteins due to the presence of its three *tatA* genes, a mutant strain (total-*tat*) lacking all known *B. subtilis tat* genes was constructed. This was achieved in three subsequent steps (schematically represented in Fig. 1): first, the *tatAc* gene was disrupted with an erythromycin resistance marker (resulting in the strain Δ*tatAc*); second, the *tatAy-tatCy* operon was replaced with a spectinomycin resistance marker (resulting in the strain Δ*tatAc*-Δ*tatAyCy*); and third, the *tatAd-tatCd* operon was replaced with a chloramphenicol resistance marker (resulting in the total-*tat* strain). The fact that the total-*tat* mutant strain could be constructed shows that a functional Tat pathway is not essential for viability of *B. subtilis*, at least not under laboratory conditions when cells are grown in rich or minimal media at 37 °C (data not shown). Furthermore, the total-*tat* mutation did not inhibit the development of natural competence for DNA-binding and uptake, sporulation, and subsequent spore germination (data not shown), showing that these developmental processes do not require a functional Tat translocation apparatus.

The Extracellular Proteome of B. subtilis Total-tat—As a first approach to study the effects of the total-*tat* mutation on the composition of the extracellular proteome, the proteins secreted into the growth medium under conditions of phosphate starvation were analyzed by two-dimensional gel electrophoresis. The results showed that, under these conditions, the composition of the extracellular proteome of the total-*tat* mutant was indistinguishable from that of the Δ*tatCd*-Δ*tatCy* mutant (data not shown). This confirmed our previous observation that PhoD is secreted in a strictly Tat-dependent manner, representing ~8–10% of the extracellular proteome (6). Notably, relatively few proteins are secreted under conditions of phosphate starvation (36). Therefore, the two-dimensional gel electrophoretic analysis was also performed with postexponentially growing cells in rich medium, which are known to secrete the largest number of different proteins as compared with exponentially growing cells in rich medium or phosphate-starved cells (4). A representative result is shown in Fig. 2, in which dual channel imaging was used to monitor possible changes in extracellular protein composition. Strikingly, none of the detectable extracellular proteins was completely absent from the growth medium of the total-*tat* mutant. It has to be noted that some protein spots (labeled in green), which correspond to proteins that have not yet been identified, appear to be absent from the medium of the total-*tat* strain. In other independent experiments these spots were, however, detectable in the medium of the total-*tat* mutant. Conversely, proteins (labeled in red) that appear to be absent from the medium of the parental

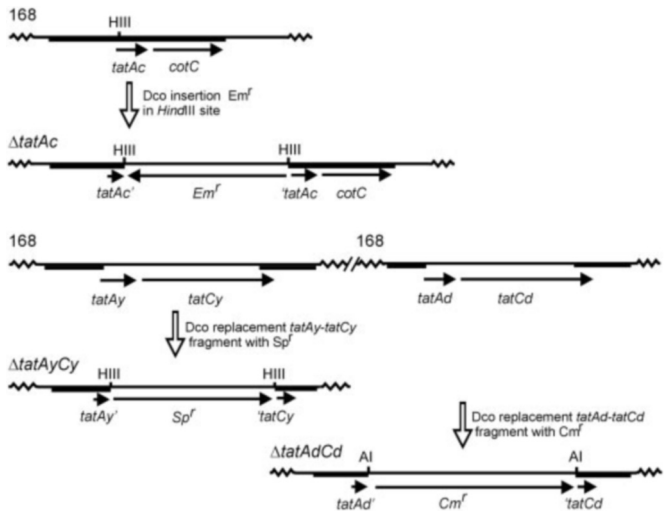

FIG. 1. **Construction of the total-*tat* mutant strain of *B. subtilis*.** Schematic representation of the construction of *B. subtilis* Δ*tatAc*, *B. subtilis* Δ*tatAyCy* and *B. subtilis* Δ*tatAdCd*. The chromosomal *tatAc* gene was disrupted with an erythromycin resistance marker (Em^r) by double crossover (dco) recombination. To this purpose, *B. subtilis* 168 was transformed with plasmid pJKAc4, which cannot replicate in *B. subtilis* and contains a disrupted copy of the *tatAc* gene with a Em^r marker in the unique *Hin*dIII site. The chromosomal *tatAy-tatCy* operon was replaced with a spectinomycin resistance marker (Sp^r) by double crossover recombination. To this purpose, *B. subtilis* 168 was transformed with plasmid pRACy3, which cannot replicate in *B. subtilis*, and contains a mutant copy of the *tatAy-tatCy* operon with large parts of the *tatAy* and *tatCy* genes replaced by a Sp^r marker. The chromosomal *tatAd-tatCd* operon was replaced with a chloramphenicol resistance marker (Cm^r) by double crossover recombination. To this purpose, *B. subtilis* 168 was transformed with plasmid pRACd5, which can not replicate in *B. subtilis*, and contains a mutant copy of the *tatAd-tatCd* operon with large parts of the *tatAd* and *tatCd* genes replaced by a Cm^r marker. PCR-amplified DNA fragments that were used to direct integration of resistance markers into the *B. subtilis* chromosome are indicated with *black bars* (for details: see "Experimental Procedures"). Only restriction sites relevant for the construction are indicated. HIII, *Hin*dIII; AI, *Acc*I; *tatAc'*, 3′-truncated *tatAc* gene; *'tatAc*, 5′-truncated *tatAc* gene; *tatAy'*, 3′-truncated *tatAy* gene; *'tatCy*, 5′-truncated *tatCy* gene; *tatAd'*, 3′-truncated *tatAd* gene; *'tatCd*, 5′-truncated *tatCd* gene.

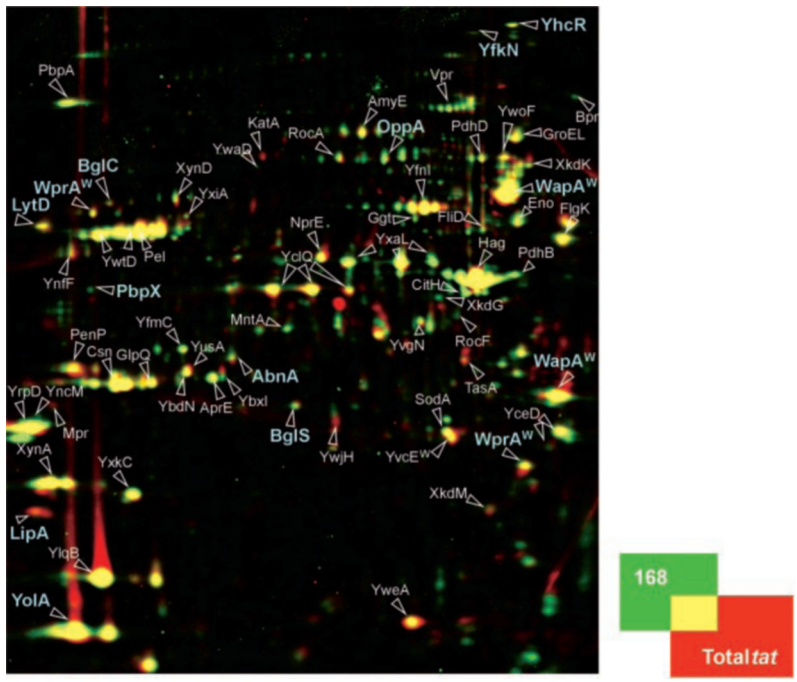

FIG. 2. **The extracellular proteome of *B. subtilis* 168 and total-*tat*.** Cells of *B. subtilis* 168 and the total-*tat* strain were grown in rich medium and extracellular proteins were collected 1 h after entry into the stationary phase. Secreted proteins were analyzed by two-dimensional gel electrophoresis and dual channel fluorescence imaging as indicated under "Experimental Procedures." *Green protein spots* are predominantly present in the master image of the extracellular proteins of *B. subtilis* 168; *red protein spots* are predominantly present in the image of the extracellular proteins of the *B. subtilis* total-*tat* strain; and *yellow protein spots* are present at similar amounts in both images. The present picture was obtained by dual channel imaging of two representative warped two-dimensional gels on which extracellular proteins of the parental strain and the total-*tat* mutant were separated, respectively. Notably, the composition of the extracellular proteome of each strain was investigated in three independent experiments. The names of proteins identified by MALDI-TOF mass spectrometry are indicated, and the names of proteins with predicted RR/KR signal peptides are marked in *blue*.

strain 168, and present in the medium of the total-*tat* mutant, were detectable in independent experiments using the medium of the parental strain. These variations must, therefore, be attributed to the natural dynamics in the composition of the extracellular proteome. Of the 64 extracellular proteins identified by MALDI-TOF mass spectrometry, the LipA, PbpX, WprA, WapA, YfkN and YhcR proteins were predicted to be synthesized with RR-signal peptides (Table I). In addition, six proteins that were predicted to contain KR-signal peptides were identified. These are AbnA, BglC, BglS, LytD, OppA, and YolA (Fig. 2). Taken together, these observations imply that, within the detection limits of two-dimensional gel electrophoresis, PhoD is the only known protein of *B. subtilis* for which a strictly Tat-dependent accumulation in the growth medium can be demonstrated.

Different Effects of tatC Mutations on the Extracellular Accumulation of LipA—The signal peptide of LipA conforms very well to the most stringent criteria that are currently available for the prediction of RR-signal peptides. These include the presence of hydrophobic residues at the +2 *and* +3 positions relative to the twin-arginines, and a hydrophobic H-domain with an average hydrophobicity of less than 2.1 (Table I; Refs. 9 and 37). It was, therefore, remarkable that the extracellular accumulation of LipA was not affected by the total-*tat* mutation (Fig. 2). This prompted us to investigate the secretion of LipA in more detail. For this purpose, various *tat* mutant strains were grown in rich medium and the amount of extracellular LipA was examined by Western blotting. Surprisingly, the extracellular accumulation of LipA was affected by *tatCd* mutations, but not by a *tatCy* mutation (Fig. 3), or mutations in the *tatA* genes (data not shown). Nevertheless, LipA remained detectable in the medium of all *tat* mutant strains, showing that its secretion is not strictly Tat-dependent.

Tat-independent Secretion of LipA—As the levels of LipA

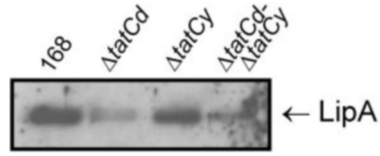

FIG. 3. **TatCd-dependent extracellular accumulation of the *B. subtilis* lipase LipA.** *B. subtilis* 168, *B. subtilis* Δ*tatCd*, *B. subtilis* Δ*tatCy* and *B. subtilis* Δ*tatCd*-Δ*tatCy* were grown in rich medium until 1 h of postexponential growth. To study the extracellular accumulation of LipA, *B. subtilis* cells were separated from the growth medium by centrifugation. Proteins in the growth medium were concentrated 20-fold by precipitation with trichloroacetic acid, and samples for SDS-PAGE were prepared. LipA in the growth medium was visualized by SDS-PAGE and Western blotting using LipA-specific antibodies.

synthesis in the parental strain 168 are low and do not allow the analysis of the LipA secretion process by pulse-chase labeling experiments, further studies on the secretion of this protein were performed with LipA overproducing strains containing the plasmid pLip2031 (38). As shown by two-dimensional gel electrophoresis, the Δ*tatCy*-Δ*tatCd*(Cm) double mutation did neither affect the extracellular accumulation of overproduced LipA when the cells were grown in rich medium (Fig. 4*A*), nor under conditions of phosphate starvation (Fig. 4*B*). Similarly, the extracellular accumulation of AbnA, BglC, BglS, LytD, OppA, PbpX, WapA, WprA, YdhF, YfkN, YhcR, and YolA, which are synthesized with potential RR/KR-signal peptides (Table I), remained unaffected by the absence of TatCd and TatCy (Fig. 4, *A* and *B*). Furthermore, irrespective of the presence or absence of TatCd and TatCy, the overproduction of LipA did not affect the general composition of the extracellular proteome (Fig. 4; data not shown). In contrast to LipA, PhoD was absent from the medium of phosphate-starved Δ*tatCy*-Δ*tatCd*(Cm) mutant cells containing pLip2031 (Fig. 4*B*), which was a predictable observation as PhoD is secreted in a TatCd-

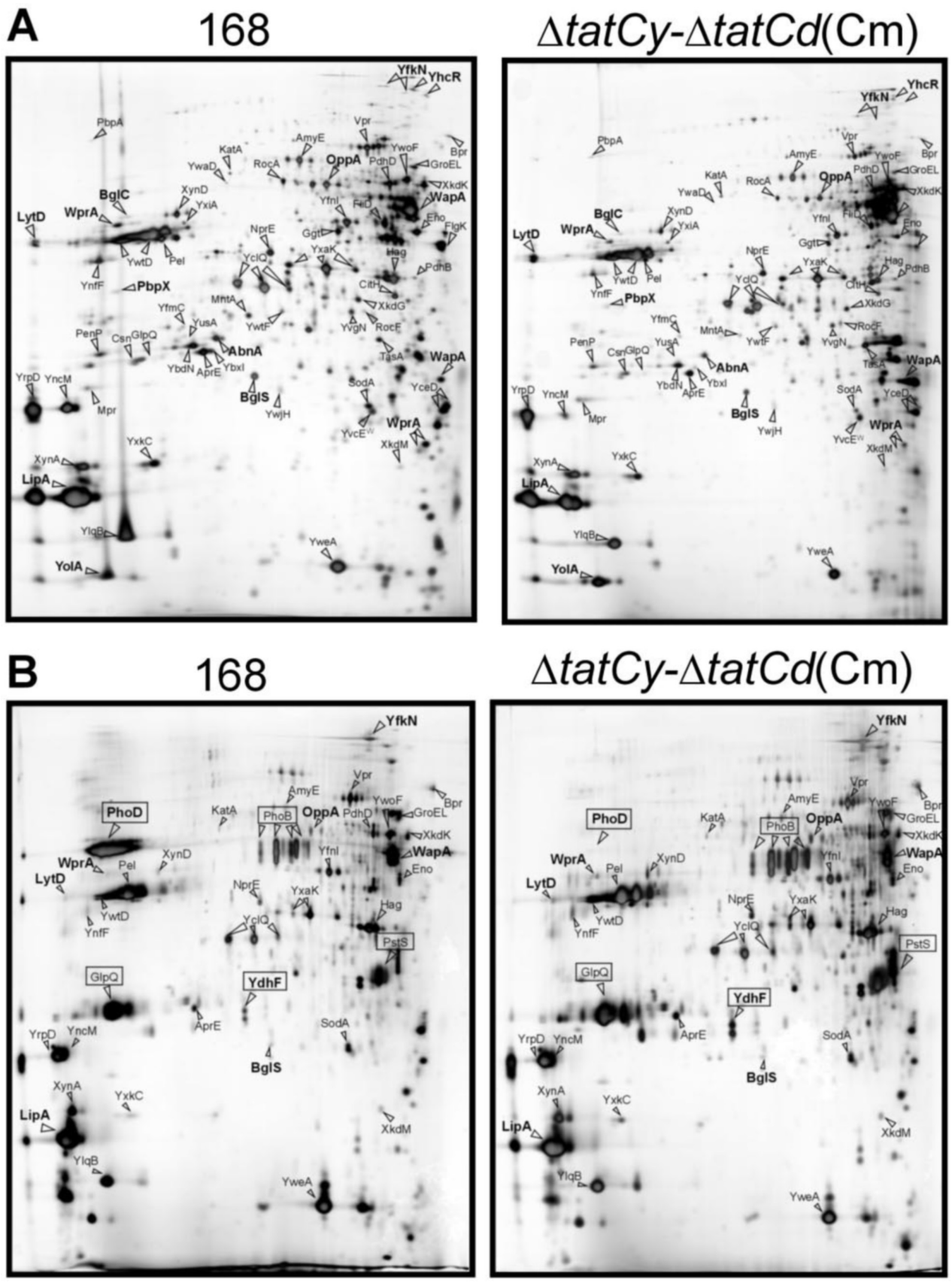

FIG. 4. **Two-dimensional gel electrophoretic analysis of the extracellular proteome under conditions of LipA overproduction.** *B. subtilis* 168 and *B. subtilis* Δ*tatCy*-Δ*tatCd*(Cm), both of which were transformed with plasmid pLip2031 for high-level production of LipA, were grown in rich medium (*A*) or under conditions of phosphate starvation in LPDM (*B*). Secreted proteins were analyzed by two-dimensional gel electrophoresis as described under "Experimental Procedures." The names of proteins identified by MALDI-TOF mass spectrometry are indicated. The names of proteins that are predicted to contain RR/KR-signal peptides are printed in bold, and the names of proteins expressed as a result of phosphate starvation (*panel B*) are indicated by *boxes*. Please note that, due to overloading with LipA, the high pH range of the gels in *panel A* (*left side* of each gel) is distorted. Consequently, LipA is present as a double spot.

TABLE III
LipA activity

To determine the esterase activity of extracellular LipA, cells of *B. subtilis* 168, Δ*tatCd*(Cm), Δ*tatCy*, Δ*tatCy*-Δ*tatCd*(Cm) and total-*tat* overproducing LipA from plasmid pLip2031, or wild type strain 168 (no LipA overproduction) were grown overnight. Cells and medium were separated by centrifugation and 50 μl of culture supernatant was used for esterase activity determinations (for details: see "Experimental Procedures"). The numbers represent average values of experiments performed in duplicate, using four different pLip2031 transformants per strain. LipA activities are indicated as the increase in the absorbance at 405 nm · min^{-1}·OD_{600}.

Strain	Activity
168 (no pLip2031)	0.04 ± 0.01
168 (pLip2031)	0.48 ± 0.02
Δ*tatCd*(Cm) (pLip2031)	0.45 ± 0.08
Δ*tatCy* (pLip2031)	0.47 ± 0.09
Δ*tatCy*-Δ*tatCd*(Cm) (pLip2031)	0.31 ± 0.05
total-*tat* (pLip2031)	0.49 ± 0.08

dependent manner (6). The conclusion that the extracellular accumulation of overproduced LipA is not significantly affected by *tatC* mutations was confirmed by Western blot experiments (data not shown) and LipA activity determinations (Table III) using *tatCy* and *tatCd* single and double mutant strains, as well as the total-*tat* mutant. Finally, the correct processing of LipA in the Δ*tatCy*-Δ*tatCd*(Cm) and total-*tat* mutants was verified by N-terminal sequencing of mature LipA that was isolated from the growth media of these strains. Like the mature LipA in the growth medium of the parental strain 168, LipA in the media of multiple *tat* mutant strains started with the sequence Ala-Glu-His-Asn-Pro-Val (data not shown). This implies that pre-LipA is indeed processed at the previously predicted type I signal peptidase cleavage site between residues 31 and 32 (2). Taken together, these observations show that the secretion of overproduced LipA is not significantly affected by the absence of a functional Tat pathway, and that the Tat-independently secreted LipA is correctly processed and folded into an active conformation.

SecA-dependent Secretion of Overproduced LipA—The Sec-dependent pathway of *B. subtilis* can be regarded as the major route for protein secretion into the growth medium (2, 39). Therefore, we investigated whether the Tat-independently secreted LipA was transported in a Sec-dependent manner. For this purpose, plasmid pLip2031 was introduced in the *B. subtilis* strain I*secA*, which contains an IPTG-inducible *secA* gene. Next, the processing of LipA by signal peptidase, which requires the translocation of pre-LipA across the membrane, was analyzed by pulse-labeling experiments using SecA-depleted cells. These were obtained by growing *B. subtilis* I*secA* overnight in S7 medium supplemented with IPTG. Subsequently, these cells were washed, resuspended and grown in fresh S7 medium without IPTG until they reached an OD_{600} of 0.6. The cells thus depleted for SecA were used for pulse-labeling. In parallel, the parental strain 168 and the total-*tat* mutant, both containing plasmid pLip2031, were subject to the same growth regime and used for pulse labeling. As shown in Fig. 5, the processing of pre-LipA to the mature form was strongly affected by SecA depletion (reduced synthesis of SecA was monitored by SecA immunoprecipitation). In contrast, the absence of a functional Tat machinery had no effect on this process. These results were confirmed by pulse-chase labeling, showing that the rate of the conversion of pre-LipA to the mature form was significantly slowed down upon SecA depletion, but not in the total-*tat* mutant (data not shown). It has to be noted that the different strains used for pulse-labeling incorporated different amounts of ^{35}S-labeled methionine and cysteine (data not shown). As shown by the immunoprecipitation of the control protein GroEL, these differences in label incorporation account for the different amounts of labeled LipA in Fig. 5. Interestingly, the processing of the α-amylase AmyQ of *B. amyloliquefaciens*, which is known to be secreted in a Sec-dependent manner (40), was neither affected by reduced levels of SecA synthesis nor the total-*tat* mutation. This was demonstrated using cells transformed with plasmid pKTH10, which directs the overproduction of AmyQ (Fig. 5). Consistent with the observed processing of AmyQ, SecA depletion under the present conditions does not result in the complete absence of the SecA protein from *B. subtilis* I*secA* (data not shown), despite the fact that the rate of SecA synthesis is strongly reduced (Fig. 5).

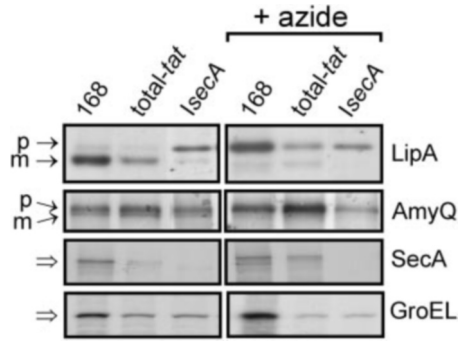

FIG. 5. **SecA-dependent processing of LipA.** Processing of pre-LipA or pre-AmyQ (Sec-dependent control protein) was analyzed in the *B. subtilis* strains 168, total-*tat* and I*secA*. These strains were either transformed with plasmid pLip2031 for high-level LipA production, or plasmid pKTH10 for high-level AmyQ production. Cells were labeled for 1 min with [^{35}S]methionine/cysteine at 37 °C as indicated under "Experimental Procedures." Subsequently, specific antibodies were used for the precipitation of LipA, AmyQ, SecA, or GroEL. The immunoprecipitated proteins were analyzed by SDS-PAGE and fluorography. When required, sodium azide (final concentration: 1.5 mM) was added 5 min prior to labeling (+ azide). SecA and GroEL were precipitated from samples of pulse-labeled *B. subtilis* strains containing pLip2031. It has to be noted that the different strains used for pulse labeling incorporated different amounts of [^{35}S]-labeled methionine and cysteine. *p*, pre-LipA or pre-AmyQ; *m,* mature LipA or AmyQ; ⇒, SecA, or GroEL.

To verify the Sec-dependence of LipA secretion in the total-*tat* mutant, the translocation ATPase activity of SecA was inhibited with sodium azide. For this purpose, cells of *B. subtilis* total-*tat*, I*secA* or the parental strain 168 were subject to the growth regime described above. However, 5 min prior to labeling with [^{35}S]methionine/cysteine the cells were incubated with 1.5 mM sodium azide. As shown in Fig. 5, pre-LipA processing was sensitive to sodium azide both in the total-*tat* mutant and the parental strain 168. Similarly, the processing of pre-AmyQ to the mature form was sensitive to sodium azide in cells of *B. subtilis* 168, *B. subtilis* total-*tat*, and *B. subtilis* I*secA* depleted of SecA (all of which were transformed with pKTH10 for AmyQ production). Taken together, the pulse-labeling experiments indicate that the translocation of pre-AmyQ and pre-LipA across the membrane is blocked in the presence of sodium azide, which implies that these preproteins are exported in a SecA-dependent manner. However, pre-LipA translocation is more sensitive to SecA depletion than pre-AmyQ translocation, which indicates that the export of LipA requires higher cellular levels of SecA than the export of AmyQ.

Proteomic Evaluation of Sec-dependent Protein Secretion—Previous proteomic studies by Hirose *et al.* (39) suggested that the secretion of the majority of extracellular proteins by *B. subtilis* is strongly SecA-dependent. However, the interpretation of these results was complicated by the fact that a temperature-sensitive *secA* mutant strain was used, which stops growing and dies upon temperature upshift. Furthermore, a limited number of extracellular proteins were identified in

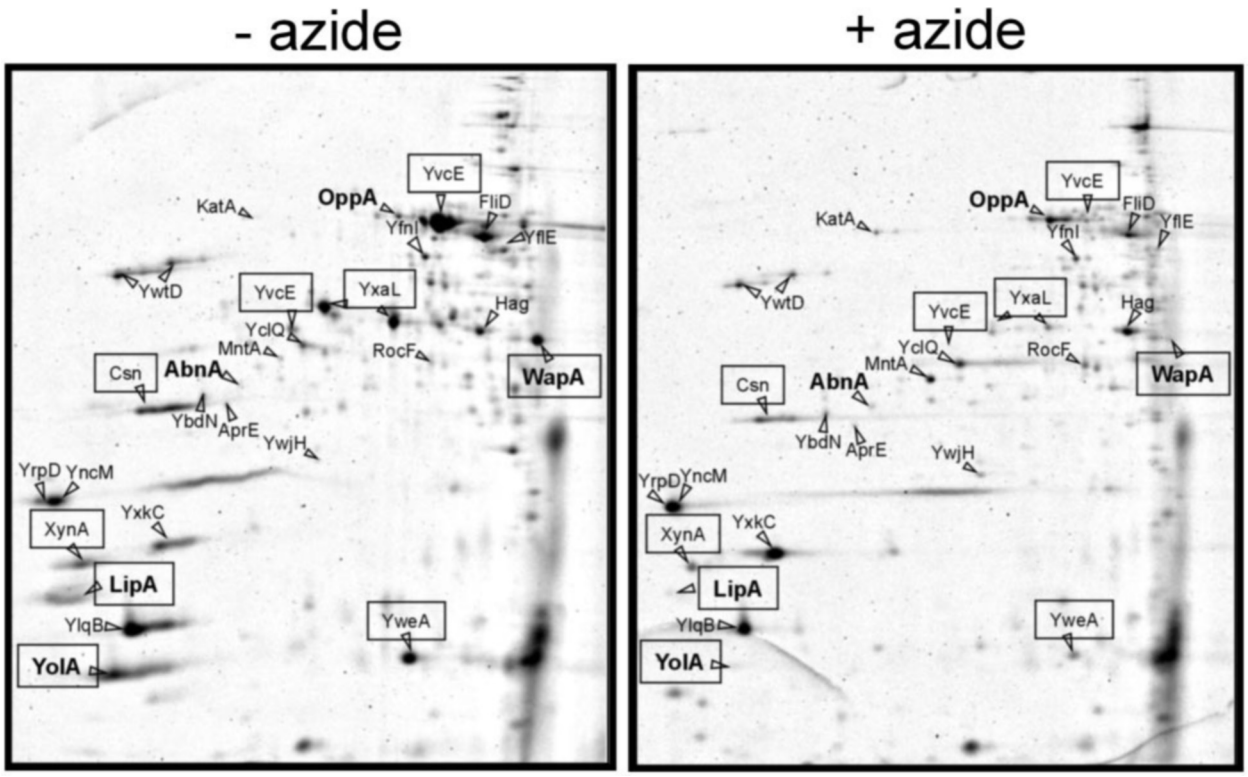

FIG. 6. **Effects of sodium azide on the secretion of *de novo* synthesized extracellular proteins of *B. subtilis* 168.** Cells of *B. subtilis* 168 were grown in rich medium to an OD_{540} of 3.0. Next, cells were separated from the growth medium, washed, resuspended in prewarmed fresh medium and divided into two separate cultures, one of which was supplemented with 15 mM sodium azide. After 20 min of growth, the proteins secreted into the medium were analyzed by two-dimensional gel electrophoresis as indicated under "Experimental Procedures." Protein spots identified by MALDI-TOF mass spectrometry are indicated. The names of proteins that are predicted to contain RR/KR-signal peptides are printed in *bold*, and those of proteins of which the secretion is reduced in the presence of sodium azide are *boxed*.

these studies, which included only two (WapA and WprA; Ref. 39) of the 14 proteins with predicted RR/KR-signal peptides that could be visualized in the present studies. Therefore, a different approach, based on the use of sodium azide, was followed to investigate the SecA dependence of protein secretion by *B. subtilis* 168 at a proteomic scale. For this purpose, it was essential to study the secretion of *de novo* synthesized proteins because, otherwise, kinetic effects of sodium azide on protein secretion would be overshadowed by the large amounts of extracellular proteins that accumulate in the growth medium of this strain. Thus, postexponentially growing *B. subtilis* cells were separated from the (rich) growth medium, washed, and resuspended in fresh medium, with or without sodium azide. Next, the proteins secreted into the medium within 10 or 20 min of growth were analyzed by two-dimensional gel electrophoresis. This procedure resulted, in particular, in the visualization of those extracellular proteins that normally accumulate in the growth medium at relatively high levels (Fig. 6; only the 20-min samples are shown). Of the 26 identified *de novo* synthesized proteins that can be detected in the medium of cells that were not treated with sodium azide, a subset was secreted at reduced levels when the cells were grown in the presence of sodium azide. These azide-sensitive extracellular proteins are: Csn, LipA, WapA, XynA, YolA, YvcE, YweA, and YxaL. Importantly, three of these, LipA, WapA and YolA, are synthesized with predicted RR/KR-signal peptides. While the secretion of LipA, WapA, YolA, YvcE, YweA, and YxaL was severely inhibited by azide, this inhibitor of SecA had a relatively mild effect on the secretion of Csn and XynA. In contrast, no effect of the presence of sodium azide was observed on the extracellular appearance of 18 other *de novo* synthesized proteins, which include the AbnA and OppA proteins that have predicted RR/KR-signal peptides (Table I). These observations support the view that the secretion of several proteins, including proteins with predicted RR/KR-signal peptides, depends to different extents on the activity of SecA.

DISCUSSION

Recent developments in genomics and bioinformatics provide ample possibilities to predict biochemical pathways that might be active in organisms of which the genomes have been sequenced. However, such predictions are of limited value without a biochemical or proteomic verification. In the present studies, we have used proteomic approaches to verify our previous genome-based predictions concerning the role of the Tat pathway within the so-called secretome of *B. subtilis*. By definition, the secretome includes both the pathways for protein export from the cell and the extracellular proteome (2). *B. subtilis* is an excellent model organism for a proteomic verification of predictions concerning protein export from the cytoplasm, because exported proteins are released into the growth medium unless they have retention signals that anchor them to the cytoplasmic membrane or the cell wall. Moreover, many proteins that are synthesized with membrane or cell wall retention signals end up in the growth medium due to proteolytic shaving or alternative release mechanisms (4), which allows the verification of predictions concerning their export. Our present results show that out of 69 proteins with potential RR- or KR-signal peptides (Table I), 14 can be detected on the extracellular proteome of *B. subtilis* cells grown in rich medium or under conditions of phosphate starvation. These are AbnA, BglC, BglS, LipA, LytD, OppA, PbpX, PhoD, WapA, WprA, YdhF, YfkN, YhcR, and YolA. The remaining 55 proteins were not detected in the growth medium under the laboratory conditions tested. This could be due to lack of expression of the corresponding genes (note that *phoD* and *ydhF* are only ex-

pressed under conditions of phosphate starvation), protein synthesis at levels below detection, or poor separation by two-dimensional gel electrophoresis. Alternatively, some of these 55 proteins with predicted RR/KR-signal peptides may not be exported from the cytoplasm, or may be retained in the membrane or cell wall. Indeed, these 55 proteins include 10 potential membrane proteins and 11 potential lipoproteins.

Of the 14 proteins with predicted RR/KR-signal peptides that can be detected in the growth medium, only PhoD was secreted in a strictly Tat-dependent manner as previously documented (6). In contrast, 13 detectable proteins of this category were secreted by strains containing multiple *tat* mutations, and the secretion of three of these 13 proteins (LipA, WapA, and YolA) apparently depended on SecA. Remarkably, the secretion of LipA was influenced to some extent by *tatCd* mutations, but it was not affected in the total-*tat* mutant. Consistent with the Tat-dependent extracellular accumulation of PhoD, the signal peptide of this protein conforms to the most stringent criteria for the prediction of Tat-dependence as defined for known RR-signal peptides of *E. coli* (hydrophobic residues at the +2 *and* +3 positions and a hydrophobicity of less than 2.1; Refs. 9 and 37). Strikingly, however, these stringent criteria also apply to LipA and LytD, which display a Tat-independent extracellular accumulation. This implies that the present criteria for the prediction of true RR/KR-signal peptides need to be refined, at least for *B. subtilis*. In this respect, it is important to bear in mind that the predicted RR/KR-signal peptides of the 11 remaining Tat-independently secreted proteins, which can be detected by proteomics, are imperfect. As one of these signal peptides has a highly hydrophobic H-domain (hydrophobicity of 2.3), while 10 others have non-hydrophobic residues at the +2 or +3 positions (Table I), it seems that signal peptides of *B. subtilis* should, *at least*, conform to the stringent criteria defined for RR-signal peptides of *E. coli* in order to direct Tat-dependent protein secretion.

The observation that mutations in *tatCd* reduce the amounts of LipA in the growth medium, whereas the total-*tat* mutation has no effect on the extracellular appearance of LipA, is intriguing. On the one hand, there could be a direct effect of the absence of TatCd on LipA secretion as this protein does have a potential RR-signal peptide (Table I) and can be exported via the Tat pathway of *E. coli* when fused to the RR-signal peptide of the trimethylamine N-oxide reductase TorA.[3] On the other hand, it is conceivable that the reduced levels of LipA in the medium of *tatCd* mutant cells are due to indirect effects on the synthesis of this protein. If there is a direct effect of the *tatCd* mutation on the export of LipA, this effect is clearly suppressed in the total-*tat* mutant. The Tat-independent export of LipA is particularly evident under conditions of LipA overproduction. In fact, as demonstrated by depletion of the translocation motor SecA and/or SecA inhibition with sodium azide, the export of overproduced LipA is Sec-dependent, irrespective of the absence or presence of a functional Tat machinery. As judged by the outcome of SecA depletion experiments, the translocation of pre-LipA appears to require higher cellular levels of SecA than that of pre-AmyQ, which is secreted in a strictly Sec-dependent (azide-sensitive) manner (40). This difference in SecA-requirement is reminiscent of that observed between the *B. subtilis* levansucrase SacB and the α-amylase AmyE. Compared with AmyE, the export of SacB was shown to require much higher cellular levels of SecA (41). Taken together, our observations show that LipA secretion is fully Sec-compatible. As the Sec machinery is known to transport proteins in a loosely folded conformation, it can be concluded that the folding of LipA into its active conformation can occur after its translocation across the membrane. This would be consistent with the fact that the export of active LipA does not require the Tat pathway, which can transport folded proteins. In order to refine the parameters for the prediction of Tat-dependent protein export in *B. subtilis*, we are currently investigating which changes in the LipA signal peptide are required to secrete this protein in a strictly Tat-dependent manner.

The secretion of 9 of the 26 most dominant identified extracellular proteins of *B. subtilis* is inhibited by sodium azide, indicating that their membrane translocation is powered by SecA. Of these nine proteins, six are synthesized with typical Sec-type signal peptides and three (LipA, WapA, and YolA) with predicted RR/KR-signal peptides that appear to be ignored by the Tat machinery. The latter observation shows that the lysine residues in the C-terminal regions of the signal peptides of LipA and YolA do not function as effective Sec-avoidance signals (Table I). Consistent with their apparently Sec-independent (azide-resistant) secretion, five extracellular proteins (FliD, Hag, KatA, RocF, and YwjH) lack signal peptides of a known type. Two other azide-resistant extracellular proteins, YflE and YfnI, are synthesized as integral membrane proteins, which may not necessarily require SecA for membrane translocation and subsequent processing by signal peptidases (39, 4). For example, it was previously shown that bacterial membrane proteins can be inserted into the membrane in a process that requires the Sec translocation channel components SecY, E, and G, but not SecA (42). It is presently not clear, why no effect of azide on the secretion of the ten remaining identified extracellular proteins was observed. However, eight of these ten proteins are synthesized with typical Sec-type targeting signals (2), whereas two of them (AbnA and OppA) have imperfect KR-signal peptides that resemble Sec-type signal peptides. Thus, it seems most likely that the membrane translocation of these ten proteins depends on the Sec machinery. If so, very low levels of SecA activity would be sufficient for this process.

Although PhoD represents ~8–10% of the extracellular proteome under conditions of phosphate starvation, our present observations show that, in general, the Tat pathway makes a highly selective contribution to the extracellular proteome of *B. subtilis*. At present, we can only speculate why this is the case. One possibility would be that *B. subtilis* uses the Tat pathway mainly for the export of folded (cofactor-binding) proteins, which are localized and active at the membrane-cell wall interface. This seems to apply, at least, to the iron-sulfur cluster-binding Rieske protein QcrA, which has a consensus RR-signal peptide that apparently lacks a signal peptidase cleavage site (Table I). In contrast, the Sec pathway of *B. subtilis*, which has an enormous capacity for protein secretion, would be used preferentially for the extracellular accumulation of proteins that are involved in the provision of nutrients and cell-to-cell communication. Notably, the fact that the PhoD protein is present on the extracellular proteome might argue against this possible division of tasks for the Tat and Sec pathways of *B. subtilis*. On the other hand, pre-PhoD is processed at a very low rate and substantial amounts of this protein can be detected at the membrane-cell wall interface (43). As no Tat-dependently exported proteins are detectable on the cell wall proteome of *B. subtilis* (44), it is the aim of our ongoing research to determine to what extent the Tat pathway of *B. subtilis* is involved in the biogenesis of membrane proteins.

Acknowledgments—We thank F. van der Lecq for determination of N-terminal amino acid sequences (Utrecht University Sequencing Centre, The Netherlands), M. J. Dröge for providing sera against LipA, M. Sarvas for providing sera against AmyQ, R. Freudl for providing sera against SecA, K. Binder, S. Grund, and D. Kliewe for expert technical

[3] P. G. Braun and M. J. Dröge, unpublished observations.

assistance, and H. Tjalsma, G. Venema, and members of the Export-eRRs consortium for stimulating discussions.

REFERENCES

1. Kunst, F., Ogasawara, N., Moszer, I., Albertini, A. M., Alloni, G., Azevedo, V., Bertero, M. G., Bessieres, P., Bolotin, A., and Borchert, S. *et al.* (1997) *Nature* **390,** 249–256
2. Tjalsma, H., Bolhuis, A., Jongbloed, J. D. H., Bron, S., and van Dijl, J. M. (2000) *Microbiol. Mol. Biol. Rev.* **64,** 515–547
3. van Dijl., J. M., Bolhuis, A, Tjalsma, H., Jongbloed, J. D. H., de Jong, A., and Bron, S. (2001) *Bacillus subtilis and its closest relatives* (Sonenshein, A. L., Hoch, J. A., and Losick, R., eds), pp. 337–355, ASM Press, Washington, D. C.
4. Antelmann, H., Tjalsma, H., Voigt, B., Ohlmeier, S., Bron, S., van Dijl, J. M., and Hecker, M. (2001) *Genome Res.* **11,** 1484–1502
5. Tjalsma, H., Kontinen, V. P., Prágai, Z., Wu, H., Meima, R., Venema, G., Bron, S., Sarvas, M., and van Dijl, J. M. (1999) *J. Biol. Chem.* **274,** 1698–1707
6. Jongbloed, J. D. H., Martin, U., Antelmann, H., Hecker, M., Tjalsma, H., Venema, G., Bron, S., Dijl, J. M. van, and Müller, J. (2000) *J. Biol. Chem.* **275,** 41350–41357
7. Henry, R., Carrigan, M., McCaffrey, M., Ma, X., and Cline, K. (1997) *J. Cell. Biol.* **136,** 823–832
8. Brink, S., Bogsch, E. G., Edwards, W. R., Hynds, P. J., and Robinson, C. (1998) *FEBS Lett.* **434,** 425–430
9. Cristóbal, S., de Gier, J. W., Nielsen, H., and von Heijne, G. (1999) *EMBO J.* **18,** 2982–2990
10. Dalbey, R. E, and Robinson, C. (1999) *Trends Biochem. Sci.* **24,** 17–22
11. Berks, B. C., Sargent, F., and Palmer, T. (2000) *Mol. Microbiol.* **5,** 260–274
12. Stanley, N. R., Palmer, T., and Berks, B. C. (2000) *J. Biol. Chem.* **275,** 11591–11596
13. Hinsley, A. P., Stanley, N. R., Palmer, T., and Berks, B. C. (2001) *FEBS Lett.* **497,** 45–49
14. Molik, S., Karnauchov, I., Weidlich, C., Herrmann, R. G., and Klösgen, R. B. (2001) *J. Biol. Chem.* **276,** 42761–42766
15. Ignatova, Z., Hornle, C., Nurk, A., and Kasche, V. (2002) *Biochem. Biophys. Res. Commun.* **291,** 146–149
16. Robinson, C., and Bolhuis, A. (2001) *Nat. Rev. Mol. Cell Biol.* **2,** 350–356
17. Sargent, F., Bogsch, E. G., Stanley, N. R., Wexler, M., Robinson, C., Berks, B. C., and Palmer, T. (1998) *EMBO J.* **17,** 3640–3650
18. Bogsch, E., Sargent, F., Stanley, N. R., Berks, B. C., Robinson, C., and Palmer, T. (1998) *J. Biol. Chem.* **273,** 18003–18006
19. Sargent, F., Stanley, N. R., Berks, B. C., and Palmer, T. (1999) *J. Biol. Chem.* **274,** 36073–36082
20. Bolhuis, A., Mathers, J. E., Thomas, J. D., Barrett, C. M., and Robinson, C. (2001) *J. Biol. Chem.*, **276,** 20213–20219
21. Tjalsma, H., Bolhuis, A., van Roosmalen, M. L., Wiegert, T., Schumann, W., Broekhuizen, C. P., Quax, W. J., Venema, G, Bron, S., and van Dijl, J. M. (1998) *Genes Dev.* **12,** 2318–2331
22. Schaeffer, P., Millet, J., and Aubert, P.-J. (1965) *Proc. Natl. Acad. Sci. U. S. A.* **271,** 5463–5467
23. Müller, J. P., An, Z., Merad, T., Hancock, I. C., and Harwood, C. R. (1997) *Microbiology,* **143,** 947–956
24. Sambrook, J., Fritsch, E. F., and Maniatis, T. (1989) *Molecular Cloning: A laboratory Manual,* 2nd Ed. Cold Spring Harbor Laboratory Press, Cold Spring Harbor, NY
25. van Dijl, J. M., de Jong, A., Venema, G., and Bron, S. (1995) *J. Biol. Chem.* **270,** 3611–3618
26. Bron, S., and Venema, G. (1972) *Mutat. Res.* **15,** 1–10
27. Antelmann, H., Engelmann, S., Schmid, R., Sorokin, A., Lapidus, A., and Hecker, M. (1997) *J. Bacteriol.*, **179,** 7251–7256
28. Bradford, M. M. (1976) *Anal. Biochem.* **72,** 248–254
29. Bernhardt, J., Buttner, K., Scharf, C., and Hecker, M. (1999) *Electrophoresis* **20,** 2225–2240
30. Otto, A., Thiede, B., Müller, E. C., Scheler, C., Wittmann-Liebold, B., and Jungblut, P. (1996) *Electrophoresis*, **17,** 1643–1650
31. Laemmli, U. K. (1970) *Nature* **227,** 680–685
32. Lesuisse, E., Schank, K., and Colson, C. (1993) *Eur. J. Biochem.* **216,** 155–160
33. van Dijl, J. M., de Jong, A., Smith, H., Bron, S., and Venema, G. (1991a) *J. Gen. Microbiol.* **137,** 2073–2083
34. van Dijl, J. M., de Jong, A., Smith, H., Bron, S., and Venema, G. (1991b) *Mol. Gen. Genet.*, **227,** 40–48
35. Klein, M., Hofmann, B., Klose, M., and Freudl, R. (1994) *FEMS Microbiol. Lett.*, **124,** 393–397
36. Antelmann, H., Scharf, C., and Hecker, M. (2000) *J. Bacteriol.* **182,** 4478–4490
37. de Gier, J. W., Scotti, P. A., Saaf, A., Valent, Q. A., Kuhn, A., Luirink, J., and von Heijne, G. (1998) *Proc. Natl. Acad. Sci. U. S. A.* **95,** 14646–146451
38. Dartois, V., Copée, J. Y., Colson, C., and Baulard, A. (1994) *Appl. Environ. Microbiol.* **60,** 1670–1673
39. Hirose, I., Sano, K., Shioda, I., Kumano, M., Nakamura, K., and Yamane, K. (2000) *Microbiology* **146,** 65–75
40. Bolhuis, A., Broekhuizen, C. P., Sorokin, A., van Roosmalen, M. L., Venema, G., Bron, S., Quax, W. J., and van Dijl, J. M. (1998) *J. Biol. Chem.* **273,** 21217–21224
41. Leloup, L., Driessen, A. J. M., Freudl, R., Chambert, R., and Petit-Glatron, M. F. (1999) *J. Bacteriol.* **181,** 1820–1826
42. Scotti, P. A., Valent, Q. A., Manting, E. H., Urbanus, M. L., Driessen, A. J. M., Oudega, B., and Luirink, J. (1999) *J. Biol. Chem.* **274,** 29883–29888
43. Müller, J. P., and Wagner, M. (1999) *FEMS Microbiol. Lett.* **180,** 287–296
44. Antelmann, H., Yamamoto, H., Sekiguchi, J., and Hecker, M. (2002) *Proteomics* **2,** 591–602
45. Sipos, L., and von Heijne, G. (1993) *Eur. J. Biochem.* **213,** 1333–1340
46. Cserzo, M., Wallin, E., Simon, I., von Heijne, G., and Elofsson, A. (1997) *Protein Eng.* **10,** 673–676
47. Nielsen, H., Engelbrecht, J., Brunak, S., and von Heijne, G. (1997) *Protein Eng.* **10,** 1–6
48. Nielsen, H., Brunak, S., and von Heijne, G. (1999) *Protein Eng.* **12,** 3–9
49. Bogsch, E., Brink, S., and Robinson, C. (1997) *EMBO J.* **16,** 3851–3859
50. Kyte, J., and Doolittle, R. F. (1982) *J. Mol. Biol.* **157,** 105–132
51. Tjalsma, H., Zanen, G., Bron, S., and van Dijl, J. M. (2001) *The Enzymes* (Dalbey, R. E., and Sigman, D. S., eds) pp. 3–26, Academic Press, San Diego
52. Vieira, J., and Messing, J. (1991) *Gene* (*Amst.*) **100,** 189–194
53. Palva, I. (1982) *Gene* (*Amst.*) **19,** 81–87
54. Vagner, V., Dervyn, E., and Ehrlich, S. D. (1998) *Microbiol.* **144,** 3097–3104
55. Guérout-Fleury, A. M., Shazand, K., Frandsen, N., and Stragier, P. (1995) *Gene* (*Amst.*) **167,** 335–336
56. Wertman, K. F., Wyman, A. R., and Botstein, D. (1986) *Cell* **49,** 253–262